SAND2020-3126C
Proceedings of ASME 2020
14th International Conference on Energy Sustainability
ES2020
June 8-10, 2020, Denver, CO, USA

ES2020-1664

HIGH-TEMPERATURE PARTICLE FLOW TESTING IN PARALLEL PLATES FOR PARTICLE-TO-SUPERCRITICAL CO_2 HEAT EXCHANGER APPLICATIONS

Hendrik F. Laubscher[1, 2], Kevin J. Albrecht[1], Clifford K. Ho[1]

[1]Concentrating Solar Technologies Department
Sandia National Laboratories, Albuquerque, NM, United States
[2]hlaubsc@sandia.gov

ABSTRACT

Realizing cost-effective, dispatchable, renewable energy production using concentrated solar power (CSP) relies on reaching high process temperatures to increase the thermal-to-electrical efficiency. Ceramic based particles used as both the energy storage medium and heat transfer fluid is a promising approach to increasing the operating temperature of next generation CSP plants. The particle-to-supercritical CO_2 (sCO_2) heat exchanger is a critical component in the development of this technology for transferring thermal energy from the heated ceramic particles to the sCO_2 working fluid of the power cycle. The leading design for the particle-to-sCO_2 heat exchanger is a shell-and-plate configuration. Currently, design work is focused on optimizing the performance of the heat exchanger through reducing the plate spacing. However, the particle channel geometry is limited by uniformity and reliability of particle flow in narrow vertical channels. Results of high temperature experimental particle flow testing are presented in this paper.

Keywords: Flow uniformity, particle bridging, particle-to-sCO_2 heat exchanger, flow channels, parallel plates

INTRODUCTION

Previous studies conducted in the field of particle flow through parallel plates indicate that high temperature particle flow has great potential for the application of high temperature parallel plate heat exchangers. High temperature flow testing done in a prior study shows that a mass flow regime through a parallel plate heat exchanger can be achieved by using a 77° flow cone below the parallel plate test block [1]. High temperature particle receiver research conducted at various research institutes plays an integral part in the future of particle based heat exchangers [2]. Operating temperatures beyond 600 °C already has been proven in high temperature experimental testing for particle receivers. The DLR (Deutsches Zentrum für Luft- und Raumfahrt) recently investigated and documented the application for particle-based heat exchangers for the production of syngas by utilizing solar energy [3]. Modeling for moving packed bed particle-to-supercritical CO_2 (sCO_2) heat exchangers is the focus of recent studies and experiments conducted on a prototype test facility at the National Solar Thermal Test Facility (NSTTF) of Sandia National Laboratories [4]. Integration between the particle-based technology and sCO_2 has been demonstrated at this test facility [5]. Alternative designs for high temperature particle based heat exchangers have been investigated, focusing on alternative particle flow designs [6], [7]. A study on performance assessment of a moving packed bed heat exchanger indicates the applicability of high temperature particle based heat exchangers in the CSP industry [8]. Although numerous studies have been performed, further research in high temperature particle heat exchangers can be beneficial to industry and research institutions.

This research paper covers the study of experimental testing to identify the practical operating limits for particle flow in parallel plates at high temperature. To this end, the study's main objectives were to identify the practical limits for flow uniformity and flow stability by conducting experiments at high temperatures.

Ideally, the spacing between the plates should be as small as possible to minimize the heat diffusion length without inducing particle bridging or non-uniform flow distribution across the heat exchanger. For comparison, flow through an experimental test block was visualized through a polished quartz window at elevated temperature and at ambient temperature. High temperature testing was performed at 650 °C to mimic the actual operating condition of a particle-to-sCO_2 heat exchanger.

A set of particle channel widths (1.58 mm to 6.35 mm) was tested with sintered bauxite particles having an average diameter of 320 µm. Adjustable plate spacing was achieved by designing a reconfigurable parallel plate block. Plates with an individual thickness of 6.35 mm were used in a reconfigurable parallel plate test block for all the different channel width tests. FIGURE 1 is an illustration of the experimental setup, showing the parallel

Sandia National Laboratories is a multimission laboratory managed and operated by National Technology & Engineering Solutions of Sandia, LLC, a wholly owned subsidiary of Honeywell International Inc., for the U.S. Department of Energy's National Nuclear Security Administration under contract DE-NA0003525.

plate block and the mass flow cone. A set of spacers with uniform thickness was installed between the plates to obtain the parallel channel width for each case of channel widths. This application used standard sheet metal sizes that are available off-the-shelf and in the range of the channel widths to be experimentally tested. Since using standard, readily available materials minimized the cost of construction of this experimental setup, the use of standard materials could ultimately lower the construction cost of a utility scale parallel plate heat exchanger.

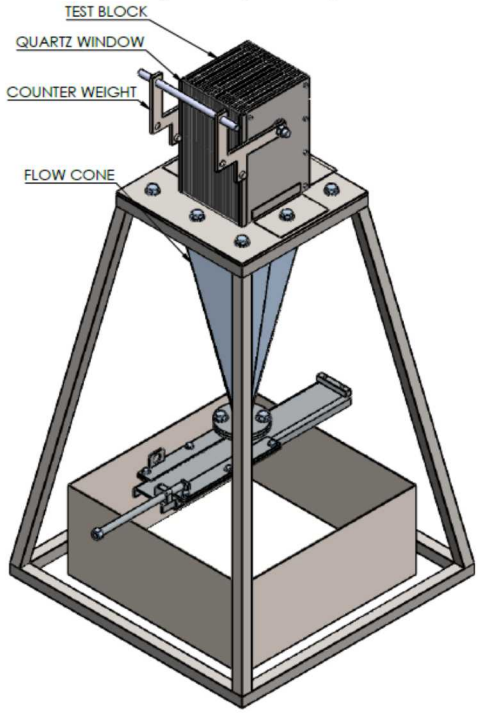

FIGURE 1: EXPERIMENTAL PARTICLE FLOW SETUP

Existing test equipment at the NSTTF was modified to achieve the reconfigurable test block used to perform the experimental testing in this study. Heating of the test setup for conducting high temperature flow testing was done in a high temperature oven, which is part of the existing facilities at the NSTTF. A summary of the channel widths investigated in this study (based on standard material sizes) is listed in TABLE 1.

TABLE 1: CHANNEL WIDTH SUMMARY FOR PARTICLE FLOW TESTING

Standard sizes	Decimal [inch]	Decimal [mm]
1/4”	0.25	6.35
3/16”	0.1875	4.76
12 GA	0.105	2.66
1/16”	0.0625	1.58

1 FLOW VISUALIZATION

1.1 Elevated temperature: 650 °C

Flow visualization of particles through a quartz window was achieved at elevated temperatures (up to 650 °C) to achieve conditions similar to the actual operating conditions of a high temperature particle-to-sCO_2 heat exchanger. High temperature particle flow testing was achieved by heating the test block in an insulated, electrically heated oven. A bulk mass of particles was heated in the oven together with the parallel plate test block. A heating period of fifteen hours was identified to be sufficient to heat the bulk particle mass as well as the stainless steel parallel plate test block to a uniform temperature of 650 °C.

During a typical high temperature flow test, the temperature at the core of the largest bulk particle mass was measured to verify that the temperature throughout the test block was at the set point temperature of 650 °C. After the temperature verification, the oven was opened and a manually operated filling mechanism filled the parallel plate test block with high temperature particles. A photograph of the test block filled with particles and at high temperature is presented in FIGURE 2.

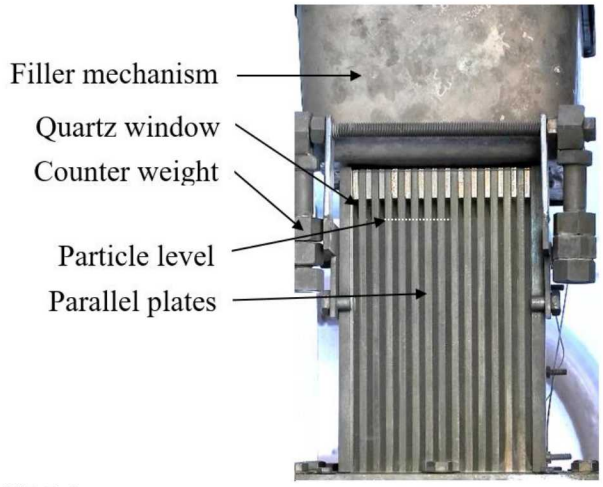

FIGURE 2: TEST BLOCK WITH QUARTZ WINDOW

A thermally induced ratcheting effect, which takes place when the parallel plate test block is heated while filled with particles, caused the quartz window to lose contact with the front edges of the parallel plates. Due to imperfections in the sealing surface and the presence of an abundance of small sphere-like particles on the interface, any small gap where a single particle could enter started the gravity driven influx of particles that was accelerated with thermal expansion. Some contamination of particles between the quartz window and the ends of the parallel stainless steel plates made conditions difficult to clearly visualize the particle levels. This phenomenon made it necessary to fill the parallel plate test block when it was already at the elevated temperature, as described in the paragraph above. Traces of particles between the quartz window and the front edges of the parallel plates are visible in the photos showing the hot flow testing for 2.66 mm channel spacing.

The flow visualization of the particles for the flowing period illustrating the different channel width sets can be seen in FIGURE 3 through FIGURE 6. The elapsed time for the captured photos in each set is indicated below each frame.

TIME: 0 SEC TIME: 9 SEC TIME: 18 SEC TIME: 27 SEC TIME: 37 SEC

FIGURE 3: HOT FLOW TESTING: 6.35 mm CHANNEL SPACING

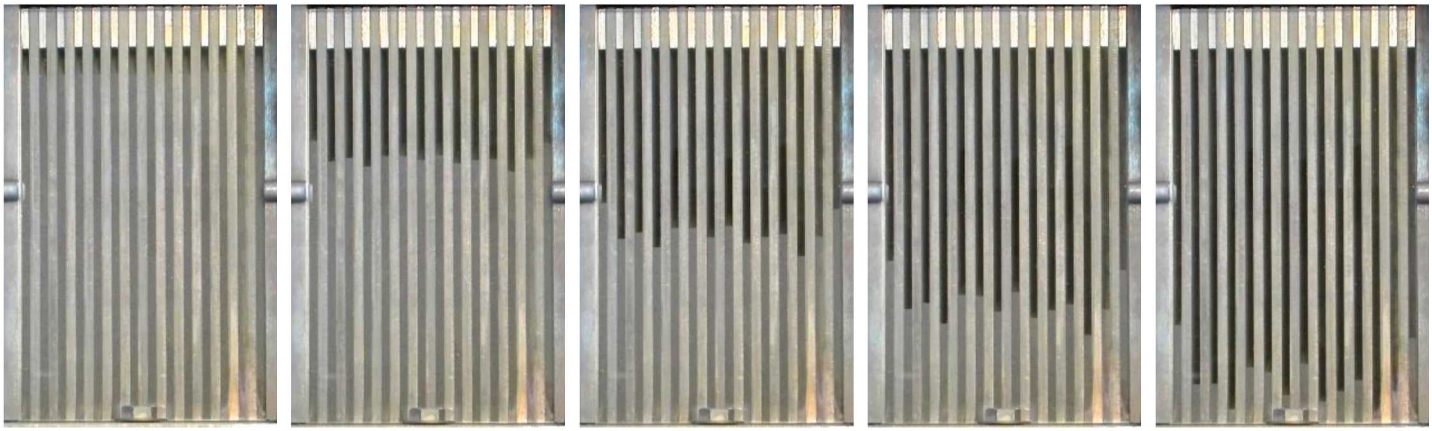

TIME: 0 SEC TIME: 12 SEC TIME: 19 SEC TIME: 26 SEC TIME: 33 SEC

FIGURE 4: HOT FLOW TESTING: 4.76 mm CHANNEL SPACING

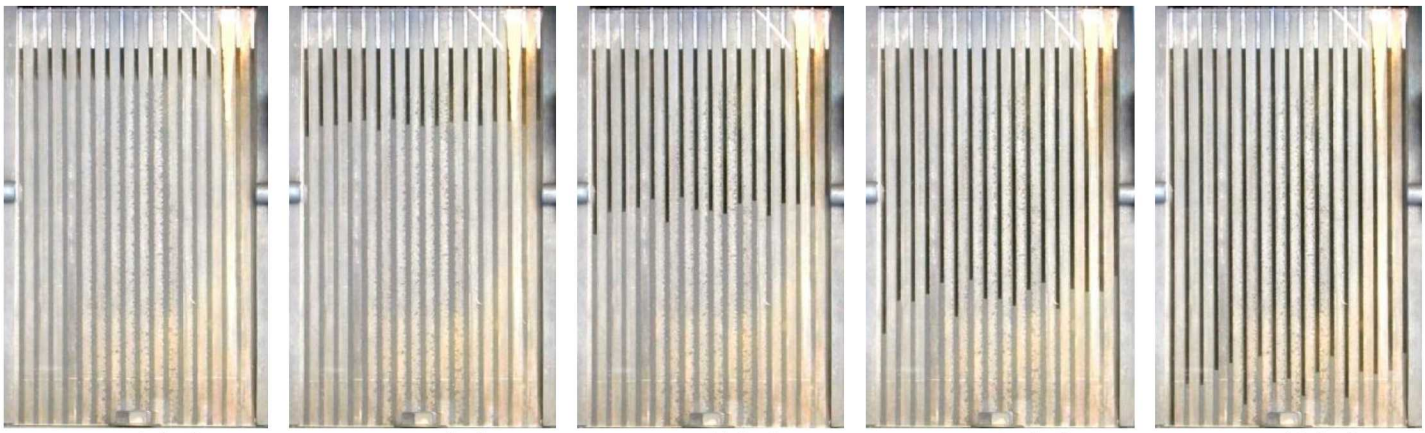

TIME: 0 SEC TIME: 5 SEC TIME: 10 SEC TIME: 15 SEC TIME: 20 SEC

FIGURE 5: HOT FLOW TESTING: 2.66 mm CHANNEL SPACING

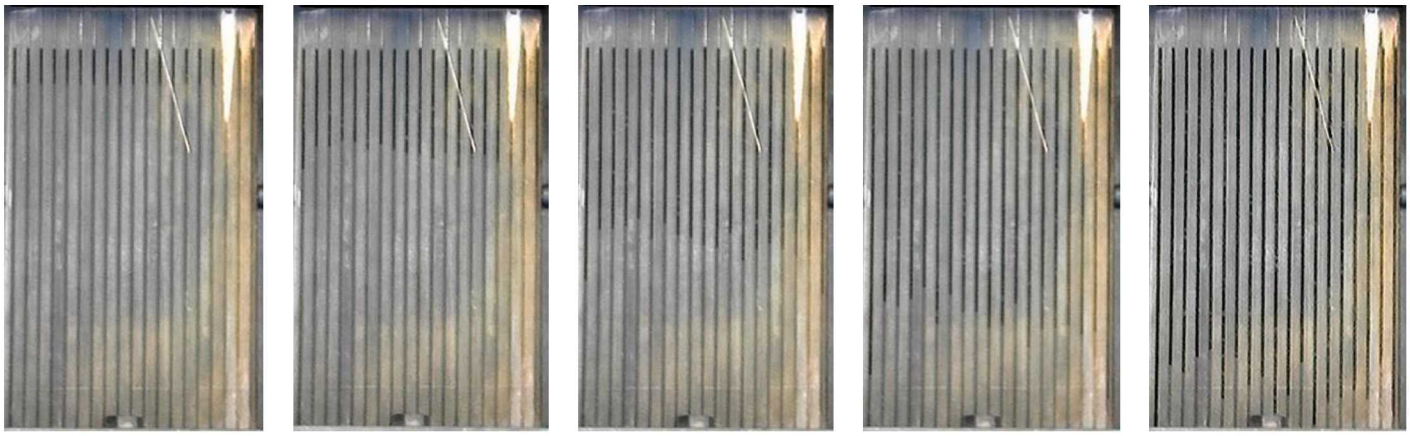

FIGURE 6: HOT FLOW TESTING: 1.58 mm CHANNEL SPACING

1.2 Ambient temperature testing: 25 °C

Ambient temperature flow visualization was done to gather benchmark data for the flow testing to compare with high temperature particle flow characteristics. The same set of channel widths between the parallel plates were experimentally tested for the ambient temperature flow test and for the high temperature flow conditions. A summary of the ambient temperature experimental results is shown in TABLE 2.

TABLE 2: FLOW DISTRIBUTION RESULTS SUMMARY FOR 25 °C TESTING

Channel Spacing	Mass Flow Variability [%]	Mass Flow [kg/s]	Flow velocity [mm/s]
1/4”	5.69	0.146	6.14
3/16”	8.95	0.147	6.77
12 GA	16.4	0.148	10.8
1/16”	18.53	0.150	18.57

2 DISCUSSION OF RESULTS

2.1 Bridging

This section discusses practical limits of when the particle flow would start forming a bridge in parallel plate channels. Flow through an experimental test block was visualized through a polished quartz window from one side only. The assumption was made that the mass flow rate over the length of the parallel plates from front to back was uniform. The particle level visible on the surface of the quartz window was thus assumed to be representative of the complete channel particle level.

Overall, both the ambient- and the high temperature particle flow testing indicated no significant bridging taking place for the given mass flow rate under investigation for any of the channel widths. The only form of bridging that was identified occurred on the end of the channel where the two walls of the channel and the quartz window meet, and this only occurred for the smallest channel spacing of 1.58 mm (0.0625 in).

This specific geometry provided the reference structure to support a particle bridge between channel walls. Bridging observed between the plates lasted only momentarily during a flow test and collapsed shorty after particle bridges were formed. A typical particle bridge consisted of four to five particles, forming an arch-like structure. A channel spacing of 1.58 mm (0.0625 in) is in the range of five individual particle diameters; therefore, the particle bridges that formed required sufficient friction on the walls of the channels and alignment of particles to form an arch. Any disturbance from the particles flowing past the newly formed bridges caused the bridges to collapse. An enlarged photograph of a residual particle bridge is presented in FIGURE 7.

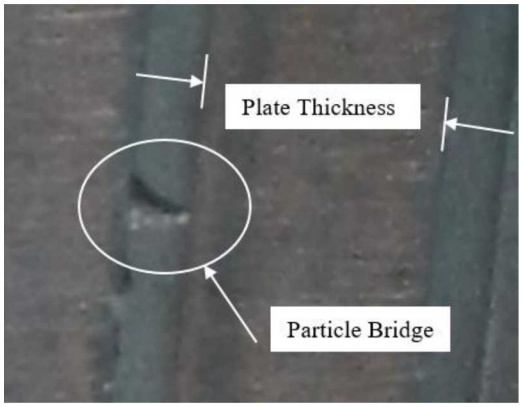

FIGURE 7: PHOTOGRAPH OF PARTICLE BRIDGE ON THE QUARTZ WINDOW WITH 1.58 mm CHANNEL SPACING

Impurities or obstructions in the flow channels were identified as a potential cause for particle bridges to form and grow. A particle bridge initiated by obstruction in the flow typically did not break down the same way as a particle-only bridge. Obstructions as a result of impurities typically found an anchor point at the leading edge of the parallel plates as the particles entered the flow section where there was a step-like geometry to rest on. Impurities that were close to the minimum channel size and entered the flow channel were likely to get wedged in at an arbitrary position with the particles in the surrounding area.

2.2 Wall effects/boundary conditions

Wall effects observed on the edge channels of the test block were seen as outliers in the data. In one scenario (4.76 mm channel width), the edge channels flowed slower than the average channel velocity. This was attributed to the interaction between the footprint of the parallel plate test block and the square opening below the test block where it led into the flow cone. In the other test scenarios, the flow in the edge channels was faster than the average flow velocity. These boundary effects observed during this experimental study were not a concern for large scale, parallel plate, moving packed bed heat exchangers because of the aspect ratio between the cross sectional flow area and the circumference length.

The wall effects on the flow of particles between parallel plates were predicted to have a much smaller effect for a larger flow setup since an experimental scale setup does not capture the large scale geometrical conditions. The aspect ratio of a large scale heat exchanger would minimize the effect of the boundaries.

2.3 Warping of plates

Heating and thermal cycling can cause slight warping of the plates during the first few thermal cycles until the plate position has settled. Heating ramp rate can also cause parallel plates to move and warp out of the design positions if the heating or cooling rates are too extreme. Parallelism between the plates also can be influenced during the manufacturing process and consequently, can cause a slight non-uniform channel width. Due to this warping or non-uniform channel spacing, the flow distribution can still fall within a 16% variability through the parallel plates as demonstrated experimentally for the 2.66 mm (0.105 in) channel spacing.

Warping of plates and non-uniform channel thickness are occurrences to be realistically expected with an actual-built heat exchanger that operates at elevated temperatures and is exposed to thermal cycling. Small manufacturing deformations or micro cracks initiated during the construction phase of a parallel plate heat exchanger can potentially cause the plates to fail at a later stage. Long term effects of plate deformation as a result of exposure to thermal cycling was not in the scope of this study.

This study documented the correlation between the non-uniform channel spacing and irregular flow distribution for the 2.66 mm channel width case. Measurements of each individual channel spacing were taken after high temperature testing and documented in the graph in FIGURE 8. This relation between the flow velocity and actual channel width shows a clear correlation. A slight inverse pattern can be identified for most of the flow channels presented in the graph. A local minimum in the flow velocity coincides with a local maximum in the channel width. Channel velocity deviation on the edges (channel 1 and 17) which represents the boundary effects discussed earlier in this paper, is not characterized in this graph. The trend line fitted on the scatter plot shows the relation between the channel width and the individual channel flow velocity.

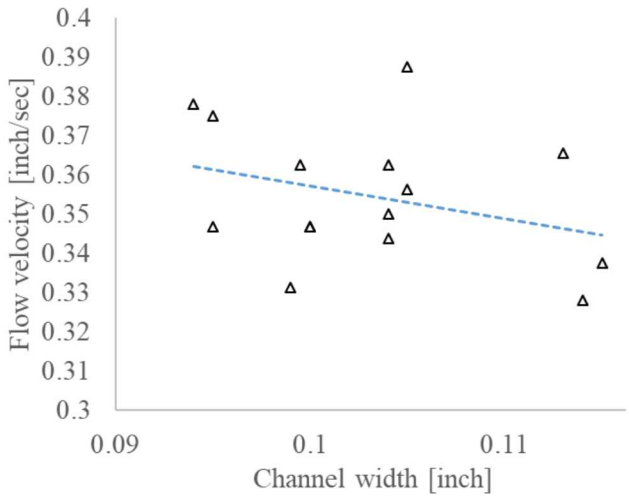

FIGURE 8: CHANNEL WIDTH VARIATION CORRELATION WITH INDIVIDUAL CHANNEL FLOW VELOCITY AFTER HIGH TEMPERATURE TESTING; 2.66 mm CHANNEL SPACING

2.4 Statistics on flow distribution

2.4.1 Data summary

A summary of the flow uniformity results indicates that an interaction between the channel walls and the particles cause an increase in flow non-uniformity as the channels become smaller. Mass flow uniformity is quantified as the percentage of variability of the flow velocity in the different individual channels.

Flow variation is calculated by making use of the equation in EQUATION 1, where V_{max} denotes the maximum flow velocity in the data group and V_{min} refers to the lowest flow velocity. For this calculation in the statistics, the outlier data of the boundary channels for each test case was not included; flow velocity data from the outlier channels skewed the results too much. The mass flow variation along the width of the test block varied from 7.75% for the largest channel spacing of 6.35 mm to 20.08% for the smallest channel spacing of 1.58 mm as tabulated in TABLE 3.

$$Flow\ variation\ (\%) = \frac{V_{max} - V_{min}}{V_{max}} \times 100 \qquad (1)$$

TABLE 3: FLOW DISTRIBUTION RESULTS SUMMARY FOR 650 °C TESTING.

Channel Spacing	Mass Flow Variability [%]	Mass Flow [kg/s]	Flow velocity [mm/s]
1/4”	7.75	0.146	5.3
3/16”	11.94	0.147	6.2
12 GA	15.32	0.146	9
1/16”	20.08	0.149	13.2

Flow velocity for the different test cases ranged from 5.3 mm/s for the 6.35 mm channel spacing to 13.3 mm/s for the 1.58 mm channel spacing. A mass flow measurement was taken for each experimental test case to ensure that the unique variation in test

conditions were taken into account when the tests were done on different days. Flow velocity was the highest through the smallest channel spacing, which created a higher friction factor for the particles. High enough flow resistance occurred for the 1.58 mm (0.625 in) test case as the packed bed started to visibly form small air voids on the surface of the quartz window as illustrated in FIGURE 9.

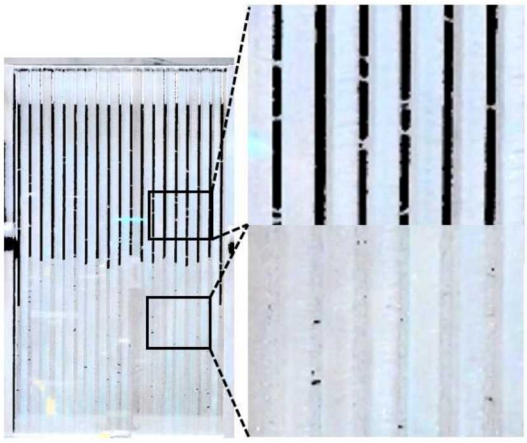

FIGURE 9: SURFACE VOIDS AND BRIDGES FORMING ON THE QUARTZ WINDOW

A safety factor should be taken into account when moving packed bed heat exchangers as they are designed to maintain continuous flow through parallel plates for a range operating conditions. During this test campaign, the limits of where such voids start to occur was identified and documented. The proposed channel width for the type of parallel plate heat exchanger in combination with the ceramic based particles investigated in this study were found to be in the range of 2.66 mm to 3.125 mm (0.105 in to 0.125 in).

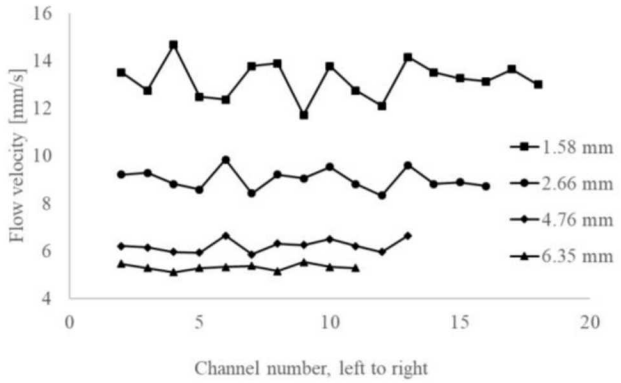

FIGURE 10: FLOW VELOCITY DISTRIBUTION FOR THE FOUR CHANNEL WIDTH CASES

2.4.2 Velocity profiles

Velocity profiles for the different flow scenarios are presented on the graph in FIGURE 10. By maintaining a constant test block width in the experimental setup for the different channel sizes, larger channel widths resulted in fewer channels in a complete test block assembly. Raw velocity values for each channel were plotted in the graph. Random flow variation over the width of the test block is shown in the line graphs, and the variation appears to be randomly distributed.

A comparison for the flow velocity of the four flow cases between ambient and elevated temperature test conditions is presented in FIGURE 11. A similar comparison for the flow variability of the four flow cases between ambient and elevated temperature test conditions is presented in FIGURE 12. These measurements show that the flow velocity difference was more noticeable at the smaller channel flow cases (cases 3 and 4). Flow cases 1 through 4 on the graphs in FIGURE 11 and FIGURE 12 are for the 6.35 mm, 4.76 mm, 2.66 mm and 1.58 mm (0.25 in, 0.1875 in, 0.105 in and 0.0625 in) cases respectively.

An overall correlation between the high temperature flow testing and the ambient temperature flow testing was observed for the flow variation. A difference of 5.4% (15.32% for the 650 °C test *vs* 9.91% for the 25 °C test) in flow variation was identified for the chosen channel spacing of 2.66 mm.

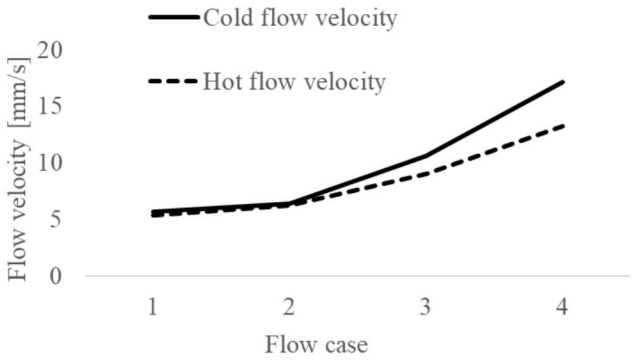

FIGURE 11: FLOW VELOCITY COMPARISON

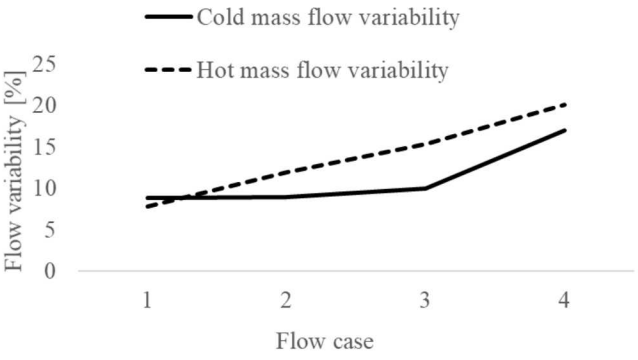

FIGURE 12: FLOW VARIABILITY COMPARISON

3 LESSONS LEARNED

3.1 High temperature filling mechanism

A filling mechanism was designed and implemented to fill the parallel plate test block while at high temperatures. The ratcheting effect that was thermally induced was largely eliminated by implementing the high temperature filling mechanism. Thermal expansion in combination with small gaps between the edges of the parallel stainless steel plates and the

quartz window were identified as the main causes for the ratcheting phenomenon.

The filling mechanism was constructed of stainless steel 316 and worked with a manually actuated lever. When the test block and the particles in the filling reservoir were heated up to a uniform 650 °C, the test block was filled, and a flow test was conducted directly thereafter. Some additional particle inventory was stored in the filling mechanism to accommodate for multiple batches of flow testing. Photographs of the filling mechanism are shown in FIGURE 13, where the filler slots are displayed in open and closed positions respectively.

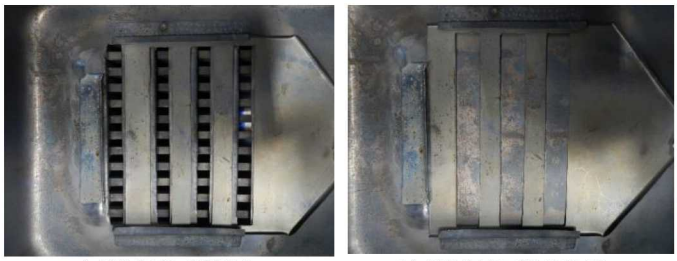

a) FILLER OPEN b) FILLER CLOSED

FIGURE 13: HIGH TEMPERATURE FILLING MECHANISM

3.2 Quartz window changing opaque

Polished quartz was used for the high temperature transparent viewing window. Quartz is thermal resistant and resists abrasion from the moving packed bed of particles, maintaining a clear vision of the moving particle bed. Some chemical reaction on the surface of the quartz started to appear after multiple high temperature testing. This caused the quartz window to turn opaque in the corners, but did not affect the main view through the majority of the window. A thin layer on the surface of the quartz window appeared affected by this and could not easily be polished out.

3.3 Flow regime for cold- *vs* hot flow

Flow through the test block at high temperature for the same mass flow setting as when calibrated at ambient temperature was slightly lower. Experimental testing indicated a faster flow through an ambient temperature test block than through a test block at high temperature. Elasticity of the particles and the stainless steel channel walls may vary with the difference in temperature and could cause higher fiction coefficients, resulting in more flow resistance.

3.4 Reconfigurable parallel plate test block

A reconfigurable test block was designed and constructed during this study. A set of 6.35 mm stainless steel plates, which resemble the heat exchanger plates, were stacked with spacers in between and bolted together to form a laminated test block with equally spaced channels in between the layers. The flow channel widths were modified by replacing the spacers with the corresponding spacers to match the new channel spacing.

Alignment of the major plates was crucial during assembly to ensure that all the surfaces of the plates on the front edge were flush in one plane. The front face of the assembled block was required to be very flat to accomplish a mechanical seal between the quartz window and the front edges of the parallel plates. The hard sphere-like ceramic based particles can cause the quartz window to separate from the front edge of the assembled test block if any particles find their way into small crevices, previously described as the ratcheting effect. For ease of reassembly, the test block was bolted together with 6.35 mm stainless steel bolts that ran through a row of holes aligning the spacers and plates.

CONCLUSION

Experimental testing was conducted at elevated temperature and at room temperature to obtain a benchmark to which the high temperature results could be compared. High temperature testing was performed at 650 °C to mimic the actual operating condition of a particle-to-sCO_2 heat exchanger. Adjustable plate spacing was achieved by design and construction of a reconfigurable parallel plate block.

The observed flow through the parallel plates showed uniform and reliable flow for the various channel widths that were tested. A flow variation of 15.32% over all the channels for the 2.66 mm case was proven experimentally. A difference in flow uniformity of 5.4% for the 2.66 mm case was identified between the low- and high temperature flow testing. Conditions for when bridging can occur were identified, and a preliminary channel spacing in the range of 2.66 mm to 3.175 mm (0.105 in to 0.125 in) was identified to provide sufficient and reliable flow uniformity while maintaining a factor of safety against bridging of particles between the plates.

Additional experimental testing is proposed for future research to capture the characteristics of different plate thickness and channel width configurations. Development and design of the optimum plate thickness would guide the design of an improved version of a parallel plate, moving packed bed heat exchanger. Motivation to develop a heat exchanger design that is cost effective to construct, easy to manufacture, and durable enough to last the lifetime of a typical CSP plant are a few of the driving factors in industry.

Experimental testing provided valuable information for channel sizing to be used in future designs of parallel plate heat exchangers for the application of particle-based CSP.

ACKNOWLEDGEMENTS

This work is funded in part or whole by the U.S. Department of Energy Solar Energy Technologies Office under Award Number 34211. This report was prepared as an account of work sponsored by an agency of the United States Government. Neither the United States Government nor any agency thereof, nor any of their employees, makes any warranty, express or implied, or assumes any legal liability or responsibility for the accuracy, completeness, or usefulness of any information, apparatus, product, or process disclosed, or represents that its use would not infringe privately owned rights. Reference herein to any specific commercial product, process, or service by trade name, trademark, manufacturer, or otherwise does not necessarily constitute or imply its endorsement, recommendation, or favoring by the United States Government

or any agency thereof. The views and opinions of authors expressed herein do not necessarily state or reflect those of the United States Government or any agency thereof.

Sandia National Laboratories is a multimission laboratory managed and operated by National Technology and Engineering Solutions of Sandia, LLC., a wholly owned subsidiary of Honeywell International, Inc., for the U.S. Department of Energy's National Nuclear Security Administration under contract DE-NA0003525.

REFERENCES

[1] K. J. Albrecht and C. K. Ho, "High-temperature flow testing and heat transfer for a moving packed-bed particle/sCO2 heat exchanger," in *AIP Conference Proceedings*, 2018, vol. 2033.

[2] H. Al-Ansary *et al.*, "On-sun experiments on a particle heating receiver with red sand as the working medium," in *AIP Conference Proceedings*, 2018, vol. 2033, pp. 1–8.

[3] C. P. Falter and R. Pitz-Paal, "Modeling counter-flow particle heat exchangers for two-step solar thermochemical syngas production," *Appl. Therm. Eng.*, vol. 132, pp. 613–623, 2018.

[4] K. J. Albrecht and C. K. Ho, "Heat Transfer Models of Moving Packed-Bed Particle-to-sCO2 Heat Exchangers," *J. Sol. Energy Eng. Trans. ASME*, vol. 141, no. 3, pp. 1–8, 2019.

[5] K. J. Albrecht, M. D. Carlson, and C. K. Ho, "Integration, control, and testing of a high-temperature particle-to-sCO2 heat exchanger," in *AIP Conference Proceedings*, 2019, vol. 2126, no. 1, p. 30001.

[6] C. K. Ho, M. Carlson, K. J. Albrecht, Z. Ma, S. Jeter, and C. M. Nguyen, "Evaluation of alternative designs for a high temperature particle-to-sCO 2 heat exchanger," *J. Sol. Energy Eng. Trans. ASME*, vol. 141, no. 2, pp. 1–8, 2019.

[7] C. Nguyen, D. Sadowski, A. Alrished, H. Al-Ansary, S. Jeter, and S. Abdel-Khalik, "Study on solid particles as a thermal medium," *Energy Procedia*, vol. 49, pp. 637–646, 2014.

[8] T. Baumann and S. Zunft, "Development and Performance Assessment of a Moving Bed Heat Exchanger for Solar Central Receiver Power Plants," *Energy Procedia*, vol. 69, no. 0, pp. 748–757, 2015.